GEOPHYSICAL RESEARCH LETTERS, VOL. 30, NO. 18, 1959, DOI:10.1029/2003GL017855, 2003

Hybrid simulations of the magnetosheath compression: Marginal stability path

Petr Hellinger and Pavel Trávníček

Institute of Atmospheric Physics, Prague, Czech Republic

André Mangeney and Roland Grappin

Observatory of Paris, Meudon, France

This paper reports a two-dimensional hybrid simulation study which utilizes an expanding box model to represent the slow compression of the plasma as it flows through the magnetosheath. In the code we model the compression as an external force: The physical sizes of the simulation box decrease with time. We present results of a simulation which starts in a parameter region of low beta where the plasma is stable with respect to both the Alfvén ion cyclotron (AIC) and mirror instabilities. In this stable region the plasma behaves double-adiabatically and an important proton temperature anisotropy appears. When the plasma becomes unstable to AIC instability, the adiabatic behavior is broken and the AIC waves keep the system close to marginal stability, the theoretical growth rate being about constant, small and positive. The AIC waves are continuously generated and the proton parallel beta increases with time. This marginal stability behavior is slightly disrupted for high proton parallel beta, where the mirror mode becomes unstable. The mirror waves rapidly grow and coexist with AIC wave, in later times the growth of AIC waves is inhibited and mirror waves become dominant. During the stages dominated by AIC and mirror waves, anticorrelation between anisotropy and proton parallel beta is observed. The hybrid expanding box simulation directly verifies the marginal stability evolution of the magnetosheath plasma.

1. Introduction

The magnetosheath plasma flow around the magnetospheric cavity exhibits large-scale inhomogeneities [*Phan et al.*, 1994; *Hill et al.*, 1995]. Their typical scale is usually much larger than the kinetic ion (and electron) scales. Therefore the magnetosheath plasma may be considered locally as homogeneous with flow-induced processes, for example a field-line stretching or a plasma compression. The double-adiabatic theory [*Chew et al.*, 1956] predicts that these processes lead to strong ion temperature anisotropies $T_\perp > T_\parallel$, where $T_\perp$ and $T_\parallel$ are the ion temperature perpendicular and parallel (with respect to the ambient magnetic field), respectively. The strong ion anisotropies $T_\perp > T_\parallel$ are not actually observed. The magnetosheath ion properties are dominated by a low-frequency turbulence transported from the shock or generated locally. The magnetosheath turbulence behind the quasi-perpendicular portion of the Earth's bow shock is relatively well understood: The turbulence is supposed to be generated mainly locally and may be regarded as a weak turbulence with different wave modes [*Lacombe and Belmont*, 1995; *Schwartz et al.*, 1996]: in low-beta plasmas transverse Alfvén ion cyclotron waves are observed whereas compressional mirror waves are observed in high-beta plasmas. All these waves are generated by the ion temperature anisotropies, and are usually observed near the marginal stability of the corresponding instability [*Anderson and Fuselier*, 1993]. As a consequence, the magnetosheath protons are characterized by an anticorrelation [*Fuselier et al.*, 1994; *Gary et al.*, 1994b] between the temperature anisotropy $T_{\perp p}/T_{\parallel p}$ and the parallel beta $\beta_{p\parallel}$

$$\frac{T_{\perp p}}{T_{\parallel p}} - 1 \sim \frac{a}{\beta_{p\parallel}^b} \tag{1}$$

where $a \sim 1$ and $b \sim 0.5$. This anticorrelation is consistent with the marginal stability relation, the linear threshold $\gamma \sim 0$, of these instabilities. The simulation studies [*Gary et al.*, 1994a; *McKean et al.*, 1994, and references therein] show that the (quasi-linear) saturation level of these instabilities follows a relation quantitatively similar to Equation (1).

These works suggest that the magnetosheath plasma follows a marginal stability path [*Manheimer and Boris*, 1977] in the ($\beta_{p\parallel}$, $A_p = T_{p\perp}/T_{p\parallel} - 1$) parameter space going from the high $\beta_{p\parallel} \sim 2$, low anisotropy $A_p \sim 0.4$ to opposite $\beta_{p\parallel} \sim 0.2$, $A_p \sim 2$ region [c.f. *Denton et al.*, 1994; *Farrugia et al.*, 2001].

In this paper we present results from a novel technique, hybrid expanding box (HEB) model, applied here in the magnetosheath context. Using this modified hybrid code we study the effect of a slow compression on the magnetosheath plasma. The simulation results directly verify the hypothesis of the marginal stability path of the magnetosheath plasma. This paper is organized as follows: Section 2 describes the HEB code, in section 3 we present the simulation results and in section 4 we discuss the results.

2. Hybrid expanding box model

In this paper we use a modified version of a 2-D hybrid code [*Matthews*, 1994], a Hybrid Expanding Box (HEB) code. The HEB code is an implementation of the expanding box model used in magnetohydrodynamic context by *Grappin et al.* [1993] to study the effects of plasma expansion on the wave evolution. The HEB code models the expansion as a linearly driven evolution where the physical lengths $\boldsymbol{x}_r$ varies with time [*Liewer et al.*, 2001; *Hellinger et al.*, 2003]. In order to study the impact of a slow compression on the magnetosheath plasma we use the same scheme, but we set $\boldsymbol{x}_r = \mathcal{L}\boldsymbol{x}$ where $\mathcal{L}$ is a diagonal matrix with

$$\mathcal{L}_{11} = 1,\ \mathcal{L}_{22,33} = 1 - t/t_c \tag{2}$$

and t_c is a characteristic time of the compression. Note the different sign in Equation (2) from that used for the expansion [*Hellinger et al.*, 2003]. The HEB code is a sophisticated version of driven hybrid simulations [*Gary et al.*, 1994b, and references therein].

The code solves the evolution of the system in the coordinates $\boldsymbol{x}$ and $\boldsymbol{v}$ co-moving with the expansion. The physical velocities $\boldsymbol{v}_r$ are $\boldsymbol{v}_r = \mathcal{L}\boldsymbol{v}$. The equation of the movement for an ion with charge q and mass m reads:

$$\frac{d\boldsymbol{x}}{dt} = \boldsymbol{v}, \quad \frac{d\boldsymbol{v}}{dt} = \frac{q}{m}(\mathcal{L}^{-1}\boldsymbol{E} + \mathcal{L}^{-2}\boldsymbol{v} \times \tilde{\boldsymbol{B}}) - 2\dot{\mathcal{L}}\mathcal{L}^{-1}\boldsymbol{v}.$$

0094-8276/05/2003GL017855$5.00

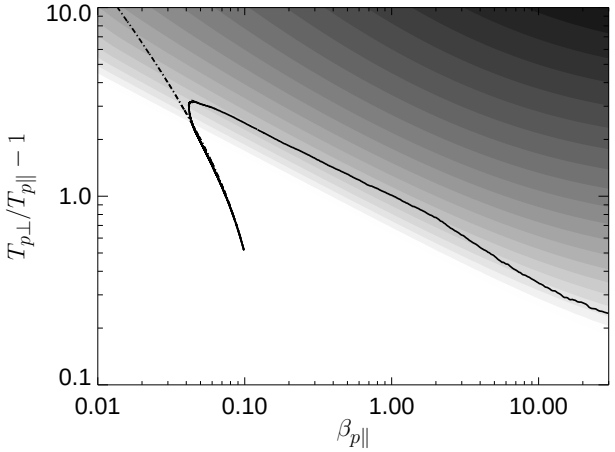

Figure 1. Evolution during the plasma compression in the space ($\beta_{p\parallel}$, $A_p = T_{p\perp}/T_{p\parallel} - 1$). The double-adiabatic prediction (Equation 3) is overplotted using dash-dotted curve. The gray-scale plot denotes linear predictions of the maximum growth rate $\gamma_{AIC} = \gamma_{AIC}(\beta_{p\parallel}, A_p)$ of the AIC instability: Darker gray denotes stronger instability whereas white corresponds to stable or marginally stable region.

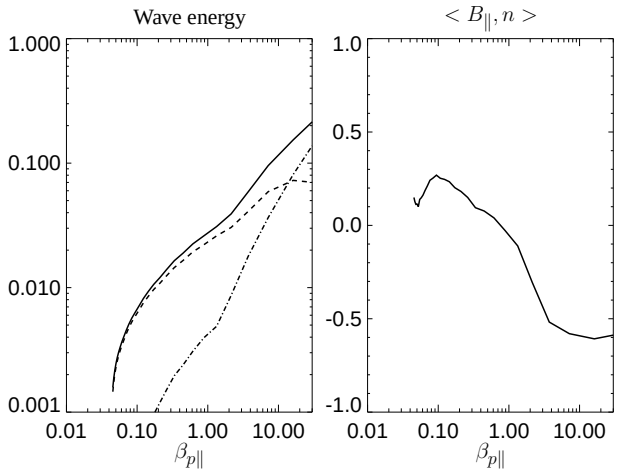

Figure 2. (left) The total fluctuating wave energy $|\delta\boldsymbol{B}|^2/B_0^2$, the fluctuating wave energy in waves with $\theta_{\boldsymbol{kB}} < 40^\circ$ (dashed curve), and the fluctuating wave energy in waves with $\theta_{\boldsymbol{kB}} > 40^\circ$ (dash-dotted curve) as a function of $\beta_{p\parallel}$. (right) Correlation between $B_\parallel$ and n as a function of $\beta_{p\parallel}$.

The effective magnetic field $\tilde{\boldsymbol{B}}$ in these coordinates evolves with the physical electric field $\boldsymbol{E}$ as $\partial\tilde{\boldsymbol{B}}/\partial t = -\mathrm{rot}(\mathcal{L}\boldsymbol{E})$ and is related to the physical magnetic field by $\boldsymbol{B} = \mathcal{L}\tilde{\boldsymbol{B}}/\det\mathcal{L}$. The electric field $\boldsymbol{E}$ is given as $\boldsymbol{E} = (\mathrm{rot}\boldsymbol{B}\times\boldsymbol{B}/\mu_0 - \boldsymbol{J}_i\times\boldsymbol{B} - \mathrm{grad}p_e)/(en)$, where μ_0 is the magnetic permeability of vacuum, n is the physical electron (and proton) number density, $n = \int f d^3\boldsymbol{v}/\det\mathcal{L}$, $\boldsymbol{J}_i$ is the proton current, $\boldsymbol{J}_i = e\int\mathcal{L}\boldsymbol{v}f d^3\boldsymbol{v}/\det\mathcal{L}$, and p_e is the electron pressure $p_e = nk_BT_e$ (k_B is Boltzman constant and T_e is the electron temperature; electrons are assumed to be isothermal).

Units of space and time are c/ω_{pi0} and Ω_{i0}, respectively, where c is the speed of light, $\omega_{pi0} = \sqrt{n_0e^2/m_p\epsilon_0}$ is the initial proton plasma frequency, and $\Omega_{i0} = eB_0/m_p$ is the initial proton gyrofrequency (B_0 is the initial magnitude of $\boldsymbol{B}$, n_0 is the initial density, e and m_p are the proton electric charge and mass, respectively; finally, ϵ_0 is the dielectric permitivity of vacuum). The code use a spatial resolution $dx = 0.25$ and $dy = 1.0$, and there are 128 particles per cell. Fields and moments are defined on a 2-D grid with dimensions 512×256. The time step for the particle advance is $dt = 0.02\Omega_{i0}^{-1}$, while the magnetic field $\boldsymbol{B}$ is advanced with a smaller time step $dt_B = dt/10$.

The initial magnetic field is $\boldsymbol{B}_0 = (B_0, 0, 0)$. During the simulation the plasma is being compressed in the y and z directions (see Equation 2). The continuous compression leads to an increase of the density and the magnitude of the magnetic field $n, B \propto 1/(1-t/t_c)^2$. In a case of slow compression one expects that the first and second adiabatic invariants are conserved [cf. *Chew et al.*, 1956], so that the proton temperature anisotropy and parallel beta evolves as

$$\frac{T_{p\perp}}{T_{p\parallel}} \propto \frac{B^3}{n^2} \propto \frac{1}{(1-t/t_c)^2},\ \beta_{p\parallel} \propto \frac{n^3}{B^4} \propto (1-t/t_c)^2. \quad (3)$$

The proton temperature anisotropy increases with time. The HEB code will show us a self-consistent reaction of the plasma to the compression when the anisotropy exceeds the threshold of the AIC and mirror instalities.

3. Simulation results

We show here the results of a simulation starting in the stable regime with respect to both the mirror and Alfvén ion cyclotron instabilities. We set $\beta_{p\parallel} = 0.1$, and proton temperature anisotropy

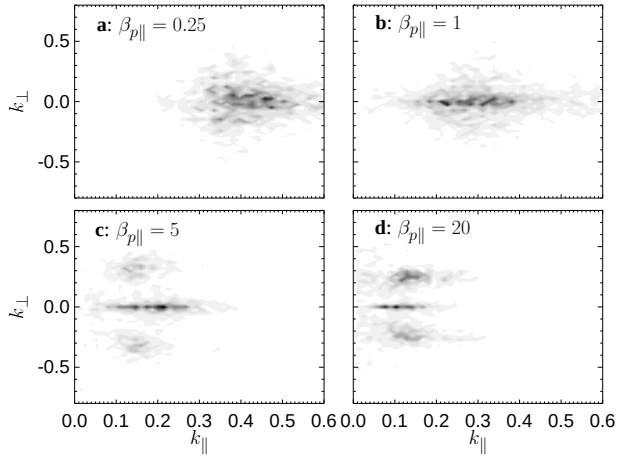

Figure 3. Spatial wave spectrum $|\delta\boldsymbol{B}|^2$ as a function of $k_\parallel$ and $k_\perp$ for different $\beta_{p\parallel}$: (a) 0.25, (b) 1, (c) 5, and (d) 20.

$T_{p\perp}/T_{p\parallel} = 1.5$ at $t = 0$. The plasma is homogeneous at time $t = 0$, except for the statistical noise due to the limited number of particles per cell.

During the simulation, the plasma is slowly compressed with the characteristic time scale $t_c = 2000\Omega_{i0}^{-1}$. The evolution of the plasma properties during the compression is shown in Figure 1. Figure 1 displays the evolution in the ($\beta_{p\parallel}$, $A_p = T_{p\perp}/T_{p\parallel} - 1$) space. The double-adiabatic prediction is overplotted using dash-dotted curve. In order to compare simulation results with the linear theory we have calculated the growth rate γ of the AIC instability in a homogeneous plasma which consists of isotropic electrons with $\beta_e = 0.1$ and of anisotropic protons for many different parameters $\beta_{p\parallel}$ and A_p. For all $\beta_{p\parallel}$ and A_p we have calculated maximum (over $\boldsymbol{k}$ vectors) growth rate γ_{AIC}. The result, $\gamma_{AIC} = \gamma_{AIC}(\beta_{p\parallel}, A_p)$, is shown in Figure 1 as a gray-scale plot: Darker gray denotes stronger instability whereas white corresponds to stable or marginally stable region.

The evolution may be split into three phases. During the first phase, the plasma is stable with respect to the AIC/mirror instabilities, and evolves double-adiabatically in agreement with Equation 3. The double-adiabatic evolution (Equation 3) translates into

an upward motion in the ($\beta_{p\|}$, A_p) space of Figure 1. This evolution leads to the development of an important proton temperature anisotropy, which crosses the threshold for the AIC instability (Figure 1, gray scale plot). Then starts the second phase of the evolution where the generated waves heat the plasma and keep the system near the marginal stability. The system follows the condition

$$\gamma_{AIC} \sim 0.08\Omega_i. \quad (4)$$

During the second phase, the system follows the path described by *Gary et al.* [1994a].

The third phase is characterized by a departure from the relation $\gamma_{AIC} \sim \text{const}$. The transition takes place in the region $\beta_{p\|} \sim 0.5 \div 1$. During the second and third phases, the fluctuating wave energy $|\delta \boldsymbol{B}|^2/B_0^2$ increases with $\beta_{p\|}$. Figure 2 (left panel) shows the total fluctuating wave energy (solid curve), the fluctuating wave energy in waves with $\theta_{\boldsymbol{kB}} < 40^\circ$ (dashed curve), and the fluctuating wave energy in waves with $\theta_{\boldsymbol{kB}} > 40^\circ$ (dash-dotted curve) as a function of $\beta_{p\|}$. There is an important increase of $|\delta \boldsymbol{B}|^2/B_0^2$ in the transition region $\beta_{p\|} \sim 0.5 \div 1$. This transition is connected with the development of mirror instability (the oblique waves, see left panel of Figure 2, dash-dotted curve).

Let us now check that the oblique waves have properties of the mirror waves: A correlation $< B_\|, n >$ between the parallel component of magnetic field $B_\|$ and the density n is negative for mirror waves whereas for AIC waves this quantity is positive [cf. *Lacombe and Belmont*, 1995]. Figure 2 (right panel) displays the dependence of the correlation $< B_\|, n >$ on $\beta_{p\|}$ during the second and third phases. Figure 2 (right panel) shows that $< B_\|, n >$ is positive during the second phase and becomes negative in the third phase. This anticorrelation is a clear signature of the mirror waves.

During the second phase, the wave spectrum is dominated by the AIC waves, whereas during the third phase the mirror becomes the dominant mode. The transition between the two phases is smooth and for a wide range of $\beta_{p\|}$ the two modes coexist. Figure 3 shows the spatial spectrum $|\delta \boldsymbol{B}|^2 = |\delta \boldsymbol{B}(k_x, k_y)|^2$ for different $\beta_{p\|}$. The k vectors are given in units of ω_{pi}/c (where ω_{pi} is the local plasma frequency $\omega_{pi} = (n_0 e^2/m_p \epsilon_0)^{1/2}$). Note, that the second and third phases are characterized by an anticorrelation between A_p and $\beta_{p\|}$. During these two phases we have

$$A_p \sim 1.1 \beta_{p\|}^{-0.5}. \quad (5)$$

4. Discussion and Conclusion

We have presented the first results of the hybrid expanding box model in the magnetosheath context. Using the 2-D HEB simulations, we have investigated the effect of a slow compression on the plasma and low-frequency turbulence. The compressed plasma initially evolves double-adiabatically as long as the plasma is stable with respect to the Alfvén ion cyclotron instability.

Later on, the AIC waves appear with relatively low amplitudes. The low amplitude AIC waves are able to keep the plasma-waves system close to the marginal stability criterion of the AIC instability in agreement with the quasilinear theory [*Gary et al.*, 1993b]. The trajectory in the ($\beta_{p\|}$, A_p) space for $\beta_{p\|} \lesssim 3$ may be expressed as $\gamma_{AIC} \sim 0.08\Omega_i$, where γ_{AIC} is the maximum linear growth rate of the AIC instability in a homogeneous (bi-Maxwellian) plasma consisting of isotropic electrons and anisotropic protons. Why is the value of γ_{AIC} positive? This is probably due to the fact that the system is continuously compressed and the AIC waves are continuously generated in order to keep the system close to marginal stability. Indeed, the wave energy increases with time (and $\beta_{p\|}$). This result is in agreement with *in situ* observations [*Gary et al.*, 1993a; *Anderson et al.*, 1994] which suggest that the wave energy $|\delta \boldsymbol{B}|^2/B_0^2$ in the magnetosheath increases with $\beta_{p\|}$ and that the plasma often follows $\gamma_{AIC} \sim \text{const.} > 0$. Observations suggest different values of γ_{AIC}. The comparison of observations with the present results is difficult since the magnetosheath plasma usually contains a small abundance of alpha particles which alter the plasma properties. Moreover, the proton distribution function during the evolution deviates from the bi-Maxwellian one; the resonant interaction of protons with AIC waves produces suprathermal particles.

For $\beta_{p\|} \gtrsim 3$ the plasma path deviates from the marginal stability relation $\gamma_{AIC} \sim$ const of AIC waves. This phenomenon is not surprising since the marginal stability behavior of the AIC mode is disrupted by appearance of mirror waves. As one expects from the linear theory, the mirror instability sets on for the high-beta plasma and during this phase the AIC and mirror waves coexist. For high-beta plasmas $\beta_{p\|} \gtrsim 10$ the energy in the mirror waves exceeds the energy in the AIC waves; the growth of AIC waves is inhibited in the later stages is inhibited.

Let us now discuss the relevance of the simulation results in the magnetosheath context. The simulation results are in good agreement with predictions of the linear theory, standard and driven hybrid simulations and some observations. In the case presented, the simulation results directly verify the proposed marginal stability path. However, the simulated system goes from low-beta to high-beta plasma whereas *in situ* observations often exhibit opposite behavior [*Farrugia et al.*, 2001], especially in the near-subsolar magnetosheath and the plasma depletion layer [*Phan et al.*, 1994]. This region is characterized by an increase of magnetic field strength and a decrease of plasma density. This behavior is inaccessible to our present model which includes only compression where the magnetic field strength and the plasma density increase simultaneously. To account for the density decrease one should include to the model other important effects. For example, the field-line stretching leads typically to a decrease of proton beta [*Denton et al.*, 1994]. Our simulation model is based on a separation of temporal and spatial scales. This assumption may be violated in the magnetosheath. First, it is possible that the magnetosheath processes are faster than the typical heating scales by the AIC and mirror instabilities [*Gary et al.*, 2000]: In our simulation we investigated relatively slow compression $t_c = 2000/\Omega_{0i}$ and the characteristic heating time estimated from *Gary et al.* [2000] is about ten times smaller (for $\gamma \sim 0.1$). Second, the heated protons with high parallel velocities are able to escape along magnetic field lines. If the typical inhomogeneity scales are small, these escaping protons may not be replaced by similar protons from adjacent regions and therefore the proton parallel beta may decrease.

Despite the limitations of our model, its first results strongly support a bounded anisotropy model [*Gary et al.*, 1994a; *Denton et al.*, 1994; *Gary et al.*, 1996] and suggest that in the region dominated by a slow compression the system follow the marginal stability path from low-beta to high-beta plasma. In the future we plan to study the effect of a speed of compression: for example, there is a natural question whether the coefficient $\gamma_{AIC} \sim \text{const}$ (Equation 4) depend on the chosen value for t_c. Moreover, we want to extend our model by including the field-line stretching to elucidate the question when the plasma goes from low-beta to high-beta region and when the opposite path takes place. We also plan to consider the role of alpha particles since their presence changes the dispersive properties and growth rates of the low-frequency waves.

Acknowledgments. The authors acknowledge useful discussions with C. Lacombe and S. P. Gary. This work was supported by the grants PICS 1175 and GA AV B3042106.

References

Anderson, B. J., and S. A. Fuselier, Magnetic pulsations from 0.1 to 4 hz and associated plasma properties in the Earth's subsolar magnetosheath and plasma depletion layer, *J. Geophys. Res.*, *98*, 1461–1479, 1993.

Anderson, B. J., S. A. Fuselier, S. P. Gary, and R. E. Denton, Magnetic spectral signatures in the Earth's magnetosheath and plasma depletion layer, *J. Geophys. Res.*, *99*, 5877–5891, 1994.

Chew, G. F., M. L. Goldberger, and F. E. Low, The Boltzmann equation and the one fluid hydromagnetic equations in the absence of particle collisions, *Proc. R. Soc. London, A236*, 112–118, 1956.

Denton, R. E., B. J. Anderson, S. P. Gary, and S. A. Fuselier, Bounded anisotropy fluid model for ion temperatures, *J. Geophys. Res.*, *99*, 11,225–11,241, 1994.

Farrugia, C. J., N. V. Erkaev, D. F. Vogl, H. K. Biernat, M. Oieroset, R. P. Lin, and R. P. Lepping, Anisotropic magnetosheath: Comparison of theory with Wind observations near the stagnation streamline, *J. Geophys. Res.*, *106*, 29,373–29,385, 2001.

Fuselier, S. A., B. J. Anderson, S. P. Gary, and R. E. Denton, Inverse correlations between the ion temperature anisotropy and plasma-beta in the Earths quasi-parallel magnetosheath, *J. Geophys. Res.*, *99*, 14,931–14,936, 1994.

Gary, S. P., B. J. Anderson, R. E. Denton, S. A. Fuselier, M. E. McKean, and D. Winske, Ion anisotropies in the magnetosheath, *Geophys. Res. Lett.*, *20*, 1767–1770, 1993a.

Gary, S. P., M. E. McKean, and D. Winske, Ion-cyclotron anisotropy instabilities in the magnetosheath – theory and simulations, *J. Geophys. Res.*, *98*, 3963–3971, 1993b.

Gary, S. P., B. J. Anderson, R. E. Denton, S. A. Fuselier, and M. E. McKean, A limited closure relation for anisotropic plasmas from the Earth's magnetosheath, *Phys. Plasmas*, *1*, 1676–1683, 1994a.

Gary, S. P., M. E. McKean, D. Winske, B. J. Anderson, R. E. Denton, and S. A. Fuselier, The proton cyclotron instability and the anisotropy/beta inverse correlation, *J. Geophys. Res.*, *99*, 5903–5914, 1994b.

Gary, S. P., M. E. McKean, and D. Winske, Proton temperature anisotropy in the magnetosheath: Hybrid simulations, *Geophys. Res. Lett.*, *23*, 2887–2890, 1996.

Gary, S. P., L. Yin, and D. Winske, Electromagnetic proton cyclotron anisotropy instability: Wave-particle scattering rate, *Geophys. Res. Lett.*, *27*, 2457–2459, 2000.

Grappin, R., M. Velli, and A. Mangeney, Nonlinear-wave evolution in the expanding solar wind, *Phys. Rev. Lett.*, *70*, 2190–2193, 1993.

Hellinger, P., P. Trávníček, A. Mangeney, and R. Grappin, Hybrid simulations of the expanding solar wind: Temperatures and drift velocities, *Geophys. Res. Lett.*, *30*, 1211, doi:10.1029/2002GL016409, 2003.

Hill, P., G. Paschmann, R. A. Treumann, W. Baumjohmann, and H. Lühr, Plasma and magnetic field behavior across the magnetosheath near local noon, *J. Geophys. Res.*, *100*, 9575–9583, 1995.

Lacombe, C., and G. Belmont, Waves in the Earth's magnetosheath: Observations and interpretations, *Adv. Space Res.*, *15*, 329–340, 1995.

Liewer, P. C., M. Velli, and B. E. Goldstein, Alfvén wave propagation and ion cyclotron interaction in the expanding solar wind: One-dimensional hybrid simulations, *J. Geophys. Res.*, *106*, 29,261–29,281, 2001.

Manheimer, W., and J. P. Boris, Marginal stability analysis: A simpler approach to anomalous transport in plasmas, *Comments Plasma Phys. Controlled Fusion*, *3*, 15–24, 1977.

Matthews, A., Current advance method and cyclic leapfrog for 2D multispecies hybrid plasma simulations, *J. Comput. Phys.*, *112*, 102–116, 1994.

McKean, M. E., D. Winske, and S. P. Gary, 2-dimensional simulations of ion anisotropy instabilities in the magnetosheath, *J. Geophys. Res.*, *99*, 11,141–11,153, 1994.

Phan, T. D., G. Paschmann, W. Baumjohmann, N. Sckopke, and H. Lühr, The magnetosheath region adjacent to the dayside magnetopause – AMPTE/IRM observations, *J. Geophys. Res.*, *98*, 121–141, 1994.

Schwartz, S. J., D. Burgess, and J. J. Moses, Low-frequency waves in the Earth's magnetosheath: Present status, *Ann. Geophys.*, *14*, 1134–1150, 1996.

P. Hellinger and P. Trávníček, Institute of Atmospheric Physics, Prague 14131, Czech Republic. (Petr.Hellinger@ufa.cas.cz; trav@alenka.ufa.cas.cz)

A. Mangeney and R. Grappin, Observatory of Paris, Meudon 92190, France. (mangeney@despace.obspm.fr; Roland.Grappin@obspm.fr)